



HAL
open science

Whole-rock oxygen isotope ratios as a proxy for the strength and stiffness of hydrothermally altered volcanic rocks

Michael Heap, Valentin Troll, Chris Harris, H. Albert Gilg, Roberto Moretti, Marina Rosas-Carbajal, Jean-Christophe Komorowski, Patrick Baud

► To cite this version:

Michael Heap, Valentin Troll, Chris Harris, H. Albert Gilg, Roberto Moretti, et al.. Whole-rock oxygen isotope ratios as a proxy for the strength and stiffness of hydrothermally altered volcanic rocks. *Bulletin of Volcanology*, 2022, 84 (8), pp.74. 10.1007/s00445-022-01588-y . hal-03725509

HAL Id: hal-03725509

<https://hal.science/hal-03725509>

Submitted on 25 Nov 2022

HAL is a multi-disciplinary open access archive for the deposit and dissemination of scientific research documents, whether they are published or not. The documents may come from teaching and research institutions in France or abroad, or from public or private research centers.

L'archive ouverte pluridisciplinaire **HAL**, est destinée au dépôt et à la diffusion de documents scientifiques de niveau recherche, publiés ou non, émanant des établissements d'enseignement et de recherche français ou étrangers, des laboratoires publics ou privés.

1 Whole-rock oxygen isotope ratios as a proxy for the strength and stiffness of
2 hydrothermally altered volcanic rocks

3

4 **Michael J. Heap^{1,2*}, Valentin R. Troll³, Chris Harris⁴, H. Albert Gilg⁵, Roberto Moretti^{6,7}, Marina Rosas-**
5 **Carbajal⁵, Jean-Christophe Komorowski⁶, and Patrick Baud¹**

6

7 ¹ *Université de Strasbourg, CNRS, Institut Terre et Environnement de Strasbourg, UMR 7063, 5 rue Descartes,*
8 *Strasbourg F-67084, France*

9 ² *Institut Universitaire de France (IUF), Paris, France*

10 ³ *Department of Earth Science, Natural Resources and Sustainable Development (NRHU), Uppsala University,*
11 *Villavägen 16, SE-752 36 Uppsala, Sweden*

12 ⁴ *Department of Geological Science, University of Cape Town, Rondebosch 7701, South Africa.*

13 ⁵ *Department of Civil, Geo and Environmental Engineering, Technical University of Munich, Arcisstrasse 21,*
14 *80333 Munich, Germany*

15 ⁶ *Université Paris Cité, Institut de Physique du Globe de Paris, CNRS UMR 7154, F-75005 Paris, France*

16 ⁷ *Observatoire Volcanologique et Sismologique de Guadeloupe, Institut de Physique du Globe de Paris, F-97113*
17 *Gourbeyre, France*

18

19 *Corresponding author: Michael Heap (heap@unistra.fr)

20

21 ORCID

22 MJ Heap (0000-0002-4748-735X)

23 VR Troll (0000-0003-1891-3396)

24 C Harris (0000-0003-0340-6674)

25 HA Gilg (0000-0003-4304-9763)

26 R Moretti (0000-0003-2031-5192)

27 M Rosas-Carbajal (0000-0002-5393-0389)

28 J-C Komorowski (0000-0002-6874-786X)

29 P Baud (0000-0002-4728-7649)

30

31 **Abstract**

32 Hydrothermal alteration is considered to increase the likelihood of dome or flank collapse by compromising
33 stability. Understanding how such alteration influences rock properties, and providing independent metrics for
34 alteration that can be used to estimate these parameters, is therefore important to better assess volcanic hazards
35 and mitigate risk. We explore the possibility of using whole-rock $\delta^{18}\text{O}$ and δD values and water contents, metrics
36 that can potentially track alteration, to estimate the strength (compressive and tensile) and Young's modulus (i.e.
37 "stiffness") of altered (acid-sulfate) volcanic rocks from La Soufrière de Guadeloupe (Eastern Caribbean). The
38 $\delta^{18}\text{O}$ values range from 5.8 to 13.2‰, δD values from -151 to -44‰, and water content from 0.3 to 5.1 wt%. We
39 find that there is a good correlation between $\delta^{18}\text{O}$ values and laboratory-measured strength and Young's modulus,
40 but that these parameters do not vary systematically with δD or water content (likely due to their pre-treatment at
41 200 °C). Empirical linear relationships that allow strength and Young's modulus to be estimated using $\delta^{18}\text{O}$ values
42 are provided using our new data and published data for Merapi volcano (Indonesia). Our study highlights that $\delta^{18}\text{O}$
43 values can be used to estimate the strength and Young's modulus of volcanic rocks, and could therefore be used
44 to provide parameters for volcano stability modelling. One advantage of this technique is that $\delta^{18}\text{O}$ only requires
45 a small amount of material, and can therefore provide rock property estimates in scenarios where material is
46 limited, such as borehole cuttings or when sampling large blocks is impracticable.

47

48 **Keywords:** La Soufrière de Guadeloupe; Merapi; porosity; uniaxial compressive strength; tensile strength;
49 Young's modulus; whole-rock oxygen isotope ratio

50

51 **Résumé**

52 L'altération hydrothermale est considérée comme l'un des principaux facteurs augmentant les risques
53 d'effondrement du dôme ou des flancs d'un volcan et ainsi de compromettre sa stabilité. Il est donc fondamental
54 de comprendre comment l'altération influence les propriétés physiques des roches et d'identifier des marqueurs
55 permettant de la quantifier en même temps que les paramètres physiques les plus importants. Le but est de mieux
56 analyser la dynamique d'un édifice volcanique et de limiter les risques. Nous avons exploré l'utilisation des
57 mesures isotopiques $\delta^{18}\text{O}$ et δD et de la teneur en eau sur un volume de roche, mesures qui potentiellement
58 permettent de suivre l'altération (principalement par acide à sulfates), de quantifier la résistance mécanique (en
59 tension et en compression) et le module d'Young de roches altérées provenant de La Soufrière de Guadeloupe.

60 Les valeurs de $\delta^{18}\text{O}$ varient entre 5.8 et 13.2‰, alors celles de δD sont comprises entre 151 to -44‰, et la teneur
61 en eau entre 0.3 to 5.1 wt%. Il y a une très bonne corrélation entre les valeurs de $\delta^{18}\text{O}$ et la résistance mécanique
62 et les paramètres élastiques des roches mesurés en laboratoire. Ces paramètres ne varient cependant pas de façon
63 systématique avec les valeurs de δD et la teneur en eau. La compilation de données publiées sur le volcan de
64 Merapi (Indonésie) avec nos nouveaux résultats, montre que la résistance mécanique et le module d'Young
65 peuvent être estimés empiriquement à l'aide d'une simple relation linéaire en fonction des valeurs de $\delta^{18}\text{O}$. Notre
66 étude suggère par conséquent que le $\delta^{18}\text{O}$ peut être utilisé comme paramètre de bases des modèles de stabilités des
67 édifices volcaniques. L'avantage principal réside dans le fait que les mesures de $\delta^{18}\text{O}$ ne nécessitent qu'une très
68 petite quantité de roches et pourront donc permettre d'estimer les propriétés physiques des roches dans des
69 situations où les quantités de matériau accessible sont faibles, notamment quand le prélèvement de larges blocs est
70 impossible (typiquement à partir des cuttings de forages).

71

72 **1 Introduction**

73 Geophysical techniques have revealed large subsurface hydrothermal systems within active volcanoes
74 worldwide (Aizawa et al., 2009; Finizola et al., 2010; Troll et al., 2012; Rosas-Carbajal et al., 2016; Byrdina et al.,
75 2017, 2018; Ghorbani et al., 2018; Finn et al., 2018; Ahmed et al., 2018; Tseng et al., 2020; Kereszturi et al., 2021;
76 Finn et al., 2022). The hydrothermal fluids circulating within these systems can physically and chemically alter
77 the rocks (Browne, 1978), which is thought to increase the likelihood of potentially devastating dome or partial
78 edifice flank collapse by compromising their stability (Day, 1996; van Wyk de Vries et al., 2000; Reid et al., 2001;
79 Voight et al., 2002; Reid, 2004; Cecchi et al., 2004; Salaün et al., 2011; Ball et al., 2015, Rosas-Carbajal et al.,
80 2016; Ball et al., 2018; Mordensky et al., 2019; Heap et al., 2021a, b; Harnett and Heap, 2021; Darmawan et al.,
81 2022; Mordensky et al., 2022). Dome or edifice collapse can suddenly decompress pressurised hydrothermal
82 systems or gas-rich magma present at shallow depth hence triggering the formation of devastating highly mobile
83 high-energy pyroclastic density currents (blasts) exemplified by the classic 1980 eruption of Mount St. Helens
84 (USA) as well as other eruptions of varying magnitudes (Lipman and Mullineaux, 1981; Voight et al., 1981;
85 Hoblitt et al., 1981; Sparks et al., 2002; Voight et al., 2002; Boudon et al., 2005; Belousov et al., 2007; Lube et
86 al., 2012; Komorowski et al., 2013). As a result, the monitoring of hydrothermal alteration at active volcanoes,
87 and understanding how alteration influences rock physical and mechanical properties, are important to better assess
88 volcanic hazards and mitigate risk.

89 Previous experimental studies have shown that hydrothermal alteration can decrease (del Potro and
90 Hürlimann, 2009; Frolova et al., 2014; Wyering et al., 2014; Mayer et al., 2016; Farquharson et al., 2019; Heap et
91 al., 2020a, 2021a; Darmawan et al., 2022; Heap et al., 2022a) or increase (Marmoni et al., 2017; Heap et al., 2020a,
92 b, 2021b) the strength and Young's modulus of volcanic rocks. Whether alteration decreases or increases strength
93 or Young's modulus is thought to depend on (1) whether the alteration increases or decreases the porosity of the
94 rock, a factor known to exert a first-order control on the strength and Young's modulus of volcanic rocks and (2)
95 whether the alteration minerals are weaker/softer or stronger/stiffer than the primary mineral assemblage (Heap et
96 al., 2020a; Heap and Violay, 2021; Darmawan et al., 2022). Heap et al. (2021b) recently suggested that both
97 porosity-increasing and porosity-decreasing alteration could jeopardise volcano stability. These authors argued
98 that porosity-increasing alteration affects volcano stability by reducing rock strength and stiffness, whereas
99 porosity-decreasing alteration reduces permeability and increases pore fluid pressure (Heap et al., 2021b).

100 A step change in volcano hazard monitoring is possible if rock physical and mechanical properties can
101 be accurately estimated using an independent metric that quantifies alteration. Recently, Heap et al. (2021a, 2022a)
102 showed that the strength (compressive and tensile) and Young's modulus of variably altered rocks from La
103 Soufrière de Guadeloupe (Eastern Caribbean) can be estimated using the amount of alteration minerals in wt%,
104 quantified using X-ray powder diffraction (XRPD) data. Using Mt. Ruapehu (New Zealand) as a case study,
105 Schaefer et al. (2021) showed that it is possible to estimate the physical and mechanical properties of volcanic
106 rocks using rapid, non-invasive reflectance spectroscopy measurements. More recently, Darmawan et al. (2022)
107 found that the compressive strength of variably altered rocks from Merapi volcano (Indonesia) can be estimated
108 using whole-rock $\delta^{18}\text{O}$ values.

109 Whole-rock $\delta^{18}\text{O}$ values can serve as an indicator for alteration because hydrothermal processes often
110 entail an exchange of oxygen isotopes between solid igneous mineral phases and circulating fluids, or the formation
111 of new minerals such as clay minerals or sulfates (Taylor, 1974; Hansteen and Troll, 2003; Donoghue et al., 2008;
112 Berg et al., 2018). We highlight that magmatic variations in $\delta^{18}\text{O}$ values are typically small and pristine igneous
113 rocks usually have $\delta^{18}\text{O}$ ratios between 5 and 8‰ (Taylor 1974; Bindeman, 2008; Deegan et al., 2021). Indeed,
114 variations due to closed-system fractional crystallisation are usually <1‰ (Bindeman, 2008). Whole-rock $\delta^{18}\text{O}$
115 values generally increase in volcanic rocks as a function of relatively low temperature hydrothermal alteration (\leq
116 250 °C), whereas higher temperatures (≥ 400 °C) or isotopically very light meteoric waters usually tend to decrease
117 the $\delta^{18}\text{O}$ of the mineral assemblage (Taylor, 1974; Rose et al., 1994; Donoghue et al., 2010; Darmawan et al.,
118 2022). Here, we further explore the relationship between whole-rock $\delta^{18}\text{O}$ values, as well as δD values and water

119 contents, and the strength (compressive and tensile) and Young's modulus of hydrothermally altered volcanic
120 rocks. The goal of this contribution is to test whether isotopic compositions and water contents of hydrothermally
121 altered (acid-sulfate) volcanic rocks can be used to estimate their physical and mechanical properties.

122

123 **2 Materials and Methods**

124 A suite of 19 variably altered rocks from La Soufrière de Guadeloupe, an active andesitic stratovolcano
125 located on the French island of Guadeloupe in the Eastern Caribbean (Komorowski et al., 2005; Moretti et al.,
126 2020), were used for this study (sampling locations are shown in Fig. 1).

127 Volcanic unrest at La Soufrière de Guadeloupe has increased since its reawakening in 1992. This unrest is
128 manifest as the expansion of the hot outgassing area at the top of the current lava dome (which formed in CE
129 1530), the appearance of steam-dominated fumaroles and acid chloride-sulfate springs, an increase in summit and
130 flank displacement rates, an increase in the heat output from the dome, an abundance of shallow seismicity, and,
131 in April 2018, the largest felt tectonic earthquake since the last eruption in 1976–1977 (Brombach et al., 2000;
132 Villemant et al., 2005, 2014; Moretti et al., 2020; Jessop et al., 2021; Heap et al., 2021a; Moune et al., 2022). The
133 link between the stability of the volcano and a combination of hydrothermal alteration resulting from hydrothermal
134 circulation and chemical weathering due to the tropical environment has been underscored in several contributions
135 (Komorowski et al., 2005; Le Friant et al., 2006; Salaün et al., 2011, Rosas-Carbajal et al., 2016; Peruzzetto et al.,
136 2019; Heap et al., 2021a; Moretti et al., 2021; Metcalfe et al., 2021; Moune et al., 2022). As a result, La Soufrière
137 de Guadeloupe represents an ideal natural laboratory to study the influence of hydrothermal alteration on rock
138 physical and mechanical properties and volcano stability.

139 Indeed, La Soufrière of Guadeloupe is characterised by an exceptional recurrence of partial edifice collapse
140 with at least nine flank collapses that have occurred in the last 9150 years, the last of which occurred during the
141 1530 CE eruption (Komorowski et al., 2005; Boudon et al., 2007; Komorowski et al., 2012; Legendre, 2012;
142 Peruzzetto et al., 2019). Evidence from the geological record indicates that the frequency of partial edifice collapse
143 in the last 9150 years has increased compared to older eruptive episodes of the Grande Découverte volcanic
144 complex, although the collapse volume has decreased. Finally, there is a high probability that edifice collapse will
145 trigger laterally-directed explosions (between two and five of the eight edifice collapses of the last 8500 years
146 generated laterally-directed blasts) (Komorowski et al., 2005; Boudon et al., 2007; Komorowski et al., 2012;
147 Legendre, 2012; Peruzzetto et al., 2019).

148 All of the 19 blocks analysed in this study are sourced from either coherent lava blocks or coherent lavas
149 (i.e. we did not collect blocks of, for example, breccia). Of the 19 blocks collected, nine were collected from a
150 collapse scar to the northeast of dome summit (blocks H2A, H2B, H3, H4A, H5A, H6, H25, H29, and H30). Five
151 blocks were collected from the dome summit: four blocks were collected from the lava spines that protrude the
152 dome (two blocks from Cratère Sud Central, H19 and H20, and two blocks from an adjacent site, H21 and H22),
153 and one block was collected from the wall of the Lacroix Supérieur outgassing fracture on the lava dome (H18).
154 A block was collected to the southwest of dome summit from a collapse scar into a highly fractured lava that forms
155 the core of a paleo-collapse mega-block of the former volcanic edifice (WP1285). Blocks were also collected from
156 the West wall of the fault “Faille 30 août” on the lava dome (H14 and H15), and from a thick lava adjacent to the
157 Galion waterfall not associated with the CE 1530 dome (H32). The final block, a volcanic non-juvenile bomb from
158 the dome that was ejected during the 1976–1977 explosive eruption (Komorowski et al., 2005), was taken from
159 the roof of a small disused thermal bathhouse to the South of the dome summit (WP1317).

160 These rocks, previously described by Heap et al. (2021a, 2022a, b), are andesites characterised by a
161 porphyritic texture comprising magmatic phenocrysts of dominantly plagioclase and pyroxene (orthopyroxene and
162 clinopyroxene) within a microcrystalline groundmass. The mineral assemblage present in each block was
163 identified by a combination of optical microscopy, Raman spectroscopy, and X-ray powder diffraction (XRPD),
164 and quantitative phase analysis was performed using the XRPD data and Rietveld program BGMN (Bergmann et
165 al., 1998) (for more details see Heap et al., 2021a, 2022a, b). The XRPD data show that all of the rocks contain
166 variable quantities of secondary (alteration) minerals: kaolinite, alunite or natro-alunite, silica polymorphs (quartz,
167 cristobalite, tridymite, and opal-A), hematite, pyrite, gypsum, and talc (Heap et al. 2021a, 2022a, b; Table 1). The
168 predominant hydrous alteration phases are kaolinite, natro-alunite, and opal-A in these materials (Table 1)
169 suggesting fluid-rock interaction with acidic sulfate-chloride-rich fluids at relatively low temperatures (< 150–200
170 °C) (Inoue, 1995; Zimbelman et al., 2005; Scher et al., 2013; Fulignati, 2020; Heap et al., 2021a). Indeed, these
171 rocks do not contain smectite, which is not stable in highly acidic (low pH) environments. High-temperature acidic
172 alteration minerals, such as pyrophyllite, dickite, diaspore, zunyite, or topaz, are notably absent, and talc was
173 observed in only one sample (H22) in relatively low amounts (Table 1). The alteration intensity of the 19 blocks
174 from La Soufrière de Guadeloupe has been quantified in previous contributions by the weight percentage (wt%)
175 of secondary (i.e. alteration) minerals (Heap et al., 2021a, 2022a, b) and these data are available in Table 2.

176 In this contribution, we relate new whole-rock oxygen and hydrogen isotope ratio data, and H₂O
177 concentrations, with previously published data for the physical and mechanical properties of rocks from La

178 Soufrière de Guadeloupe. The uniaxial compressive strength (UCS), indirect tensile strength (ITS), and Young's
179 modulus values for multiple cylindrical samples prepared from the blocks collected from La Soufrière de
180 Guadeloupe were published in previous contributions by Heap et al. (2021a, 2022a). UCS was measured on oven-
181 dry cylindrical samples in a uniaxial load frame using a constant axial strain rate of 10^{-5} s^{-1} (Heap et al., 2021a).
182 Young's modulus, an elastic constant that describes the "stiffness" of a material, was then calculated from the
183 pseudo-linear elastic portion of the resultant uniaxial stress-strain curves (Heap et al., 2021a). ITS was measured
184 on oven-dry discs, deformed diametrically in compression using a uniaxial load frame and a constant displacement
185 rate of $0.025 \text{ mm} \cdot \text{s}^{-1}$ (Heap et al., 2022a). UCS (and therefore Young's modulus) and ITS were measured at
186 ambient laboratory pressure and temperature. These studies concluded that hydrothermal alteration, associated
187 with mineral dissolution, weak secondary minerals (such as clays), and an increase in microstructural
188 heterogeneity, resulted in a reduction in compressive strength (Heap et al., 2021a), tensile strength (Heap et al.,
189 2022a), and Young's modulus (Heap et al., 2021a).

190 Offcuts from the 19 blocks were crushed and powdered by hand, to a grain size of $\ll 1 \text{ mm}$, using a
191 ceramic pestle and mortar. The whole-rock oxygen isotope ratios of these samples were measured at the University
192 of Cape Town (South Africa) using a Thermo DeltaXP mass spectrometer (data unique to this study). Aliquots of
193 $\sim 10 \text{ mg}$ of the whole rock powders were dried overnight at $50 \text{ }^\circ\text{C}$ and then under vacuum in nickel reaction vessels,
194 then reacted with 30 kPa of CIF_3 for ~ 4 hours to extract the oxygen from silicates (Borthwick and Harmon, 1982).
195 The extracted oxygen was then converted to CO_2 by passing it over a high-temperature platinised carbon rod. For
196 full analytical details see Vennemann and Smith (1990) and Harris and Vogeli (2010). Unknowns were run with
197 duplicates of the internal quartz standard (MQ), which was used to calibrate the raw data to the SMOW (Standard
198 Mean Ocean Water) scale, using a $\delta^{18}\text{O}$ value of 10.1 for MQ (calibrated against NBS-28). The results are reported
199 in standard δ -notation, where $\delta = (\text{R}_{\text{sample}}/\text{R}_{\text{standard}} - 1) \times 1000$, R_{sample} is $^{18}\text{O}/^{16}\text{O}$ in the sample, and $\text{R}_{\text{standard}}$ is $^{18}\text{O}/^{16}\text{O}$
200 relative to SMOW (Gonfiantini, 1978). The analytical reproducibility (assumed here to be similar to the error) is
201 estimated as $\pm 0.2\text{‰}$ (2 sigma), based on long-term repeated analysis of MQ.

202 Hydrogen isotopes and water contents of the same powdered separates were determined using the method
203 of Vennemann and O'Neil (1993). Samples were first melted in quartz glass tubes using a propane torch. The raw
204 data were normalised to SMOW, and corrected for compression, using the water standards RMW ($\delta\text{D} = -131.4\text{‰}$)
205 and CTMP2010 ($\delta\text{D} = -7.4\text{‰}$) with the in-house Serina kaolinite standard analysed with the unknowns (Serina
206 bulk kaolinite, $\delta\text{D} = -57\text{‰}$, $\text{H}_2\text{O} = 12.4 \text{ wt}\%$; Harris et al., 1999). The measured δD values of the standard gave
207 an average of $-59.5 \pm 3.6\text{‰}$ (2σ , $n = 3$) after corrections to the raw data. All data were adjusted to the accepted

208 Serina kaolinite value. Water abundances (as H_2O^+) were measured from the voltage on the mass 2 collector of the
209 mass spectrometer. This was calibrated against measured volumes of standard waters analysed alongside the
210 unknowns. The measured water content of Serina kaolinite gave 12.4 wt% (± 0.5 wt% 2σ , $n = 3$) (pure kaolinite
211 has an expected water content of 13.95 wt%).

212 We compare our new data with those for Merapi volcano, collected using the same equipment and
213 techniques described above. For the samples from Merapi volcano, the compressive and tensile strength data were
214 published in Darmawan et al. (2022) and Heap et al. (2022a), respectively, the alteration data (the wt% of
215 secondary minerals, mostly sulfates) were published in Heap et al. (2019, 2022a), and the $\delta^{18}\text{O}$ values were
216 published in Darmawan et al. (2022). We have calculated the Young's modulus for the experiments presented in
217 Darmawan et al. (2022) using the pseudo-linear elastic portion of the uniaxial stress-strain curves (these data were
218 not presented in Darmawan et al., 2022).

219

220 **3 Results**

221 We find that $\delta^{18}\text{O}$ values vary from 5.8 to 13.2‰, that δD values vary from -151 to -44 ‰, and that water
222 contents range from 0.3 to 5.1 wt% for our samples from La Soufrière de Guadeloupe (Table 2). The $\delta^{18}\text{O}$ values,
223 δD values, and water content data are plotted in Fig. 2 as a function of secondary alteration mineral content in wt%
224 (Table 2), a metric used in previous studies of these materials (Heap et al., 2021a, 2022a, b). Additionally, we
225 labelled samples with a high content of sulfates (≥ 2 wt% mostly natro-alunite, rarely alunite; Table 1) and opal-
226 A (≥ 10 wt%; Table 1).

227 Although there is scatter in the data, the $\delta^{18}\text{O}$ values positively correlate with the wt% of secondary
228 minerals (Fig. 2a). We note that the two samples rich in opal-A (H20 and H21) plot slightly above the trend
229 delineated by the other data (Fig. 2a). In contrast, no simple correlation is observed for the δD values or the water
230 contents as a function of increasing wt% of secondary minerals (Figs. 2b and 2c, respectively). We highlight that
231 samples with δD values much higher or lower than the other samples are typically samples with a high sulfate
232 content (Figs. 2b). To some extent, this observation also applies to the water content data (Fig. 2c).

233 Fig. 3 shows the uniaxial compressive strength, tensile strength, and Young's modulus for samples from
234 La Soufrière de Guadeloupe as a function of $\delta^{18}\text{O}$ value, δD value, and water content. All these data are provided
235 in an Excel® spreadsheet that accompanies this contribution as Supplementary Information. The data of Fig. 3
236 show that strength (uniaxial and tensile) and Young's modulus decrease as a function of increasing $\delta^{18}\text{O}$ (Figs. 3a,

237 3d, and 3g), but it is more difficult to discern singular trends in the δD and water content data (Figs. 3b, 3c, 3e, 3f,
238 3h, and 3i).

239

240 **4 Discussion**

241 Our data show that the $\delta^{18}O$ values of variably altered rocks from La Soufrière de Guadeloupe increase
242 as a function of increasing alteration (Fig. 2a), as expected for low temperature hydrothermal alteration (≤ 250 °C)
243 (Taylor, 1974; Rose et al., 1994; Donoghue et al., 2010; Darmawan et al., 2022). The dominance of kaolinite, very
244 fine-grained natro-alunite, and amorphous silica, and the absence of smectite (Table 1), suggests alteration at
245 temperatures below 150–200 °C in a steam-heated acid sulfate alteration environment (Zimbelman et al., 2005;
246 Rye, 2005). The least altered samples have stable oxygen isotope compositions (5.8 to 7.3‰) similar to unaltered
247 andesites from La Soufrière de Guadeloupe and other volcanoes in the Eastern Caribbean (Davidson, 1985;
248 Davidson and Harmon, 1989; Van Soest et al., 2002). The highest values of about 12 ± 1 ‰, in turn, are recorded
249 for the opal-dominated altered rocks. This is consistent with the larger oxygen isotope fractionation between
250 amorphous silica and water (Kita et al., 1985) compared to alunite-water (Stoffregen et al., 1994) and kaolinite-
251 water (Sheppard and Gilg, 1996). The observed positive correlation between $\delta^{18}O$ values and percentage of
252 alteration minerals in our analysed suite can thus be interpreted as a mixing line between primary igneous isotope
253 signatures and secondary alteration phases. The scatter in the data can be explained by (1) the diversity of alteration
254 phases with their distinct oxygen isotope fractionation factors with water, (2) potential temperature variations, (3)
255 variable isotope compositions of the involved fluids, and (4) the location and the type of processes involved in the
256 alteration (e.g., alteration within the host-rock or deep-seated regions of the dome by low temperature steam
257 circulation of hydrothermal fluids in the roots of surficial fumaroles versus surficial alteration within a steaming
258 and cooling dome following emplacement).

259 In contrast to the $\delta^{18}O$ values, no simple correlation is observable for the δD values or water contents as
260 a function of increasing wt% of secondary minerals (Figs. 2b and 2c, respectively). This result is surprising due to
261 the very minor amount of primary hydrogen in these rocks, and the fact that the dominant hydrous alteration phases
262 (alunite group minerals, kaolinite) have similar nominal water contents. Based on the spurious data for samples
263 containing sulfates and/or opal-A (Figs. 2b and 2c), we suspect that the pre-treatment procedure (heating to 200
264 °C in vacuum) probably led to significant water loss in the amorphous silica phase (Brandriss et al., 1998; Martin
265 and Gailliou, 2018) and that future studies should seek alternative methods to measure similar samples. Indeed, if
266 we consider only the samples that contain minor or no sulfates and opal-A (the black symbols in Fig. 2), we observe

267 positive correlations between the δD values and water contents as a function of increasing wt% of secondary
268 minerals (Figs. 2b and 2c, respectively). This may suggest that our applied extraction technique for hydrogen
269 isotope analysis of (Na-)alunite-rich samples has released sulphur-bearing volatiles that reacted with the
270 dehydroxylation water leading to unreliable water contents and, most probably, hydrogen isotope data (see Rye et
271 al., 1992). Further, for stable hydrogen isotopes, no simple correlation with the percentage of secondary alteration
272 should be expected, as no igneous hydrous minerals were observed even in the least altered samples and the
273 hydrogen isotope composition of the altered rocks will depend on the mineral type, temperature, and water isotope
274 composition rather than simply on the wt% of secondary phases. We further note that the hydrogen isotope
275 compositions of the steam-heated acid chloride-sulfate waters will be influenced by recurrent evaporation and
276 condensation processes and thus may be quite variable (Berg et al., 2018), including positive $d^{18}O$ - dD pairs, as
277 also observed for other volcanoes in the Eastern Caribbean (Chiodini et al., 1996; Joseph et al., 2011). Furthermore,
278 the D/H fractionation factors between some of the dominant hydrous phases and water are either less well
279 constrained (e.g., alunite; Stoffregen et al. 1994) or even unknown (e.g., amorphous silica).

280 Although there are some outliers, Figs. 3a, 3d, and 3g show that the uniaxial compressive strength, tensile
281 strength, and Young's modulus of variably altered rocks from La Soufrière de Guadeloupe and Merapi volcano
282 decrease as a function of increasing $\delta^{18}O$ value. Therefore, strength and Young's modulus are decreasing as a
283 function of increasing alteration, as discussed in Heap et al. (2021a) and Darmawan et al. (2022). However, we
284 find little to no correlation between strength and Young's modulus and the δD value (Figs. 3b, 3e, and 3h) or water
285 content (Figs. 3c, 3f, and 3i), likely due to the pre-treatment of the samples at 200 °C. As noted above, the δD
286 values are not related to the wt% of secondary alteration phases, and thus alteration intensity, and the measured
287 water contents depend on the alteration mineral type. Therefore, we will focus here on using $\delta^{18}O$ as a proxy for
288 strength and Young's modulus. Although we focus here on $\delta^{18}O$ only, we do not rule out the possibility of using
289 δD and/or water contents to predict rock properties in the future, as long as alternate laboratory methods are used
290 (those that avoid pre-treating the samples at 200 °C, but can remove extraneous absorbed water).

291 Figs. 4a, 4b, and 4c show uniaxial compressive strength, tensile strength, and Young's modulus,
292 respectively, as a function of $\delta^{18}O$. The outliers in these data, shown as grey circles in Fig. 4, include samples from
293 blocks H14, H29, and H32. Blocks H14 and H29 contained mesoscale fractures, which could explain their low
294 strength and Young's modulus (Heap et al., 2021a, 2022a). Block H32, which is much stronger than the other
295 blocks (Fig. 4), was collected from an older (K-Ar age 0.079 ± 0.003 Ma; Carlut and Quidelleur, 2000), low-
296 porosity, and very thick lava adjacent to the Galion waterfall (Fig. 1). Therefore, the alteration history of this block

297 differs from the other blocks collected on, within, or adjacent to, the present-day dome that was emplaced during
298 the 1530 CE eruption nearly 500 years ago (Fig. 1). Excluding these outliers, we provide best-fit linear functions
299 to the entire dataset (La Soufrière de Guadeloupe and Merapi volcano) in Fig. 4. Uniaxial compressive strength,
300 σ_c , indirect tensile strength, σ_t , and Young's modulus, E , can therefore be estimated using the following empirical
301 equations (where strength is in MPa, Young's modulus in GPa, and $\delta^{18}\text{O}$ in ‰):

302

$$303 \quad \sigma_c = -13.8(\delta^{18}\text{O}) + 204.7 \quad (1)$$

$$304 \quad \sigma_t = -0.70(\delta^{18}\text{O}) + 13.1 \quad (2)$$

$$305 \quad E = -3.42(\delta^{18}\text{O}) + 54.0 \quad (3)$$

306

307 Estimates of the strength (compressive and tensile) and Young's modulus of volcanic rocks are required
308 in a range of laboratory- and large-scale modelling designed to understand, respectively, the mechanical behaviour
309 of volcanic rocks and the stability of volcanic flanks and domes (Watters et al., 2000; Okubu, 2004; Apuani et al.,
310 2005; Moon et al., 2005; del Potro and Hürlimann, 2008; Heap et al., 2021a, b; Heap and Harnett, 2021; Wallace
311 et al., 2021). We show here that rock physical and mechanical property estimates for volcano stability modelling,
312 important assess volcanic hazards and mitigate risk, can be provided using Eqs. (1), (2), and (3) by measuring the
313 $\delta^{18}\text{O}$ values of representative samples collected from the flank or dome of a volcano. Composite $\delta^{18}\text{O}$ -value cross-
314 sections of volcanoes (Rose et al., 1994) and $\delta^{18}\text{O}$ values determined from borehole drill cuttings (Hattori and
315 Muehlenbachs, 1982) could also be used to prepare strength and Young's modulus maps and profiles, respectively.
316 Unlike laboratory experiments, which require reasonably large blocks from which to prepare the experimental
317 samples, the approach to estimate strength and Young's modulus outlined herein, i.e. Eqs. (1), (2), and (3), requires
318 only < 1 g of material (as representative as possible; e.g., using a < 1 g aliquot of a larger mass of well-mixed
319 powdered material, if available) and is thus ideally suited to provide rock physical and mechanical property
320 estimates when only limited material is available, such as drill cuttings from boreholes or when sampling large
321 blocks is impracticable.

322 The three-dimensional structures and rock property distributions inside volcanic systems are usually
323 inferred using targeted geophysical methods. Electrical methods, such as magnetotellurics and electrical resistivity
324 tomography, have shown to be particularly useful to infer rock alteration distributions in hydrothermal systems
325 because of the influence of secondary minerals in the bulk electrical conductivity of rocks (Rosas-Carbajal et al.,
326 2016; Byrdina et al., 2018; Finn et al., 2022). Petrophysical relations that link these properties are, however, far

327 from obvious. The difficulty in establishing simple relations between electrical conductivity and the percentage of
328 alteration minerals seems to arise also from the dependence on the type of alteration (i.e. mineral composition),
329 temperature, and fluid composition (Lévy et al., 2018; Ghorbani et al., 2018), similar to what we suggest may
330 happen for whole-rock oxygen isotope. Thus, it may be interesting to compare the whole-rock oxygen isotope and
331 the electrical conductivity dependence for different degrees of altered volcanic rocks. Having both properties
332 measured for representative volcano samples could significantly improve the upscaling of the physical properties
333 measured in the laboratory to the field-scale three-dimensional models obtained by geophysical methods.

334 Although we focus here on volcanological applications, our approach could be used to provide rock
335 physical and mechanical property estimates for borehole stability assessments and stimulation strategies in
336 volcanic geothermal reservoirs, which typically comprise altered rocks (Siratovich et al., 2014; Cant et al., 2018;
337 Lévy et al., 2018). Whole-rock $\delta^{18}\text{O}$ values are also often used in mineral exploration (Green et al., 1983; Criss et
338 al., 1985; Cathles, 1993; Paradis et al., 1993; Lentz, 1999), and could therefore also be used to provide rock
339 physical and mechanical property estimates for rock drillability estimates and underground excavation stability
340 assessments during mineral exploration and extraction in volcanic terrains.

341 One drawback of our approach, however, is that our analysis (Fig. 4) has been performed on rocks that
342 show a decrease in strength and Young's modulus as a result of hydrothermal alteration (Heap et al., 2021a, 2022a;
343 Darmawan et al., 2022). However, hydrothermal alteration associated with pore- and crack-filling precipitation
344 can increase strength and Young's modulus (Marmoni et al., 2017; Heap et al., 2020b, 2021b). As a result, care
345 should be taken when using Eqs. (1), (2), and (3) to ensure that the alteration observed in a particular setting does
346 not appear to strengthen or harden the rock. Care should also be taken to ensure that the alteration is indeed low
347 temperature (≤ 250 °C) hydrothermal alteration, and that the rocks have not undergone alteration at higher
348 temperatures, which will decrease whole-rock $\delta^{18}\text{O}$ values. Therefore, a detailed study of the mineral assemblage
349 is required in order to use Eqs. (1), (2), and (3) confidently. To improve our approach to estimate rock physical
350 and mechanical properties using $\delta^{18}\text{O}$ values, more data are required for a wider variety of hydrothermally altered
351 rocks, including those with different alteration mineral assemblages (e.g., those containing smectite). We further
352 note that the analysis presented here provides laboratory-scale values of strength and Young's modulus, and so
353 these values likely require upscaling before they are used in large-scale volcano models. Strength can be upscaled
354 using, for example, the Hoek-Brown failure criterion (Hoek et al., 2002) and Young's modulus can be upscaled
355 using the Hoek-Diederichs equation (Hoek and Diederichs, 2006; Heap et al., 2020a).

356

357 **5 Concluding remarks**

358 Rock physical and mechanical properties are required for large-scale models designed to assess the
359 stability of a lava dome or volcanic flank (Watters et al., 2000; Okubu, 2004; Apuani et al., 2005; Moon et al.,
360 2005; del Potro and Hürlimann, 2008; Heap et al., 2021a, b; Heap and Harnett, 2021; Wallace et al., 2021). The
361 ubiquity of hydrothermal alteration at active volcanoes (Aizawa et al., 2009; Rosas-Carbajal et al., 2016; Byrdina
362 et al., 2017, 2018; Finn et al., 2018; Tseng et al., 2020; Kereszturi et al., 2021; Finn et al., 2022), and evidence
363 suggesting that alteration compromises volcano stability (van Wyk de Vries et al., 2000; Voight et al., 2002; Salaün
364 et al., 2011), underscores the need for not only understanding the influence of alteration on rock physical and
365 mechanical properties, but also for well constrained properties for altered volcanic rocks, data that are currently
366 rare. In certain scenarios, such as when rock blocks large enough for laboratory experiments cannot be acquired
367 (e.g., drill cuttings from boreholes, when the material is too friable or delicate to prepare samples for laboratory
368 experiments, or when it is impracticable to sample and export a sufficient number of large blocks), or when
369 laboratory equipment is not available, an independent measure of alteration that can be used to estimate the
370 required rock physical and mechanical properties would be extremely useful for routine volcano stability
371 modelling. Such a method could also be used to estimate pre-failure rock properties from semi-consolidated friable
372 material found in debris avalanches. Here we show that whole-rock $\delta^{18}\text{O}$ values, a method that requires a very
373 small amount of representative material, can be used to estimate the strength (compressive and tensile) and
374 Young's modulus of low-temperature ($\leq 150\text{-}200\text{ }^\circ\text{C}$) hydrothermally (acid-chloride-sulfate) altered dome rocks.
375 Based on the promise of the approach documented herein, we recommend that future studies further explore the
376 relationship between whole-rock $\delta^{18}\text{O}$ values and the physical and mechanical properties of altered rocks with
377 different alteration assemblies (such as those that contain smectites).

378

379 **Acknowledgements**

380 This work was supported by the TelluS Program of INSU-CNRS (“Assessing the role of hydrothermal alteration
381 on volcanic hazards”) and ANR grant MYGALE (“Modelling the phYsical and chemical Gradients of
382 hydrothermal ALteration for warning systems of flank collapse at Explosive volcanoes”; ANR-21-CE49-0010).
383 M. Heap also acknowledges support from the Institut Universitaire de France (IUF). V.R. Troll acknowledges
384 support from the Swedish Research Council (Vetenskapsrådet; grant number 2020-03789). We thank the IPGP for
385 general funding for the Observatoires Volcanologiques et Sismologiques (OVS), INSU-CNRS for the funding
386 provided to the Service National d’Observation en Volcanologie (SNOV), and the Ministère pour la Transition

387 Ecologique (MTE) for financial support for the monitoring of the unstable flank of La Soufrière de Guadeloupe.
388 We are grateful to the Parc National de Guadeloupe for allowing us to carry out geological fieldwork on La
389 Soufrière. We thank Tomaso Esposti Ongaro and Lucille Carbillet for help in the field. This study contributes to
390 the IdEx Université Paris Cité ANR-18-IDEX-0001. We thank Peter Schaaf and Ben Ellis for comments that
391 helped improve this manuscript, and Ulrich Kueppers for handling our manuscript.

392

393 **Statements and Declarations**

394 The authors declare no financial or non-financial interests that are directly or indirectly related to this work.

395

396 **Supplementary Information**

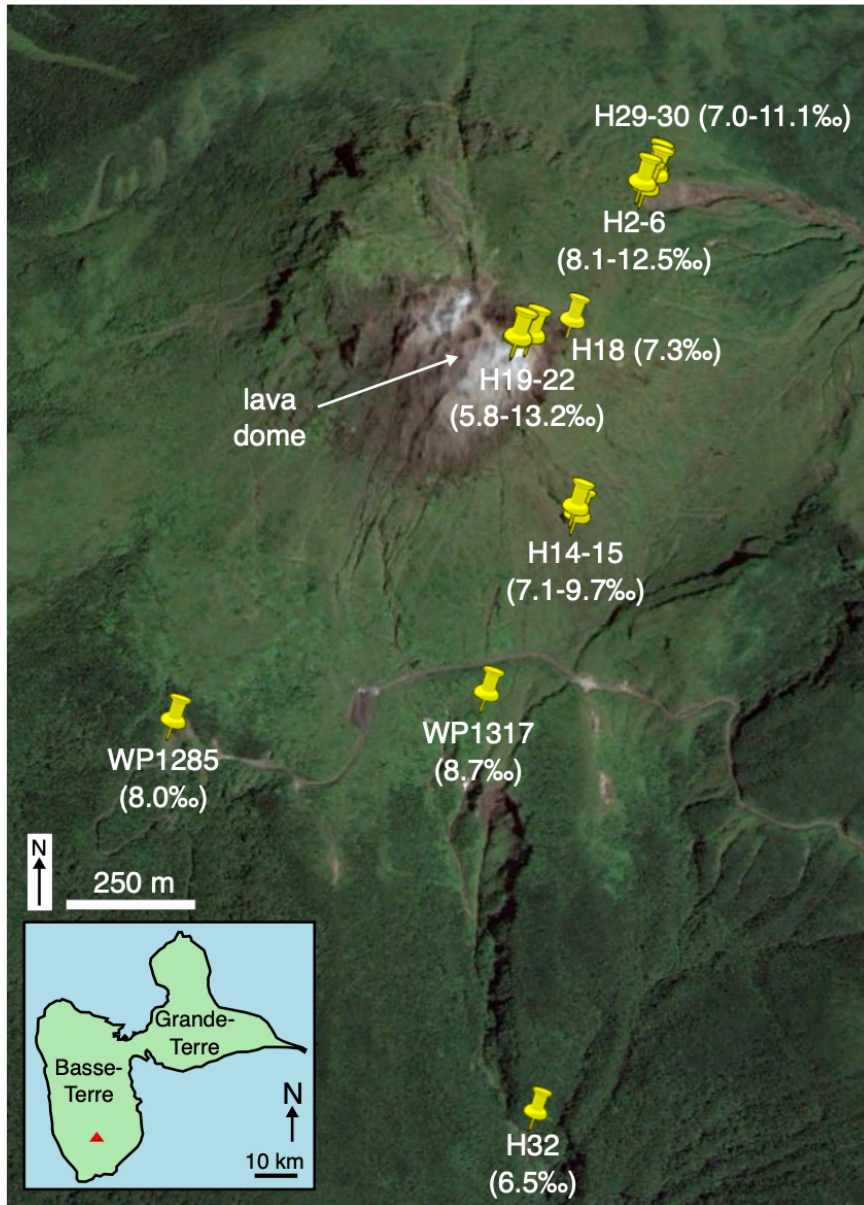
397 We provide an Excel® spreadsheet that contains the data collected for, and analysed in, this contribution.

398

399 **Author contributions**

400 Michael Heap and Valentin Troll conceived the idea for this study. Rock samples were collected by Michael Heap,
401 Marina Rosas-Carbajal, Jean-Christophe Komorowski, and Patrick Baud. Mechanical laboratory experiments were
402 performed by Michael Heap. Isotope analyses were performed by Chris Harris. Isotope data were discussed and
403 analysed by Chris Harris, Albert Gilg, Roberto Moretti, and Valentin Troll. Michael Heap wrote the manuscript,
404 with contributions from all authors. All authors read and approved the final manuscript.

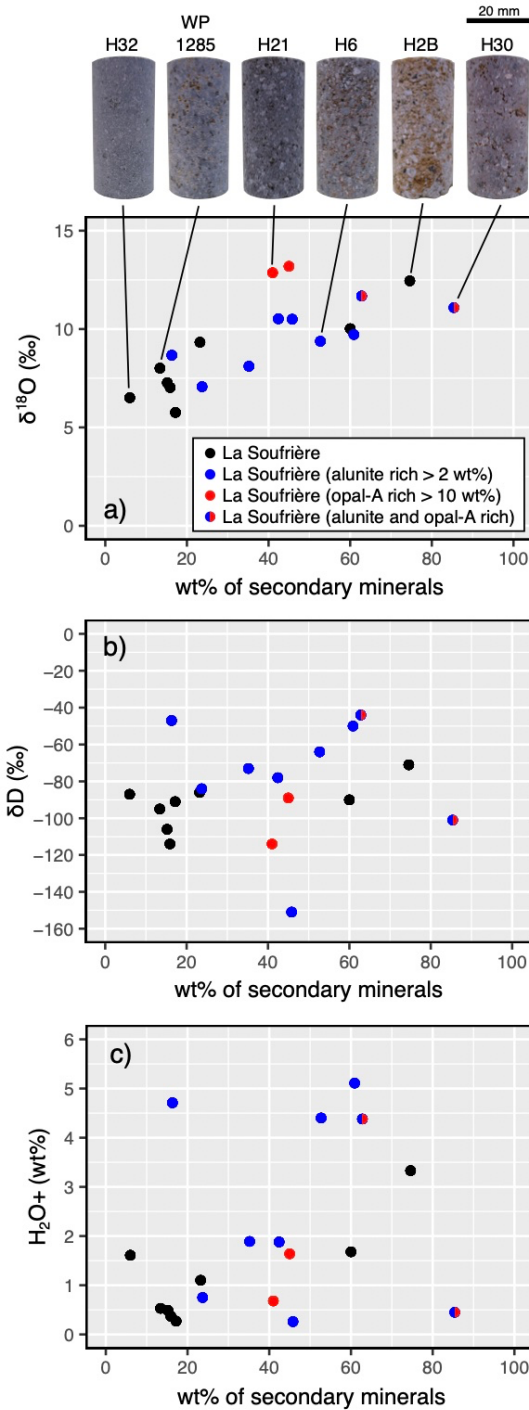
405



406

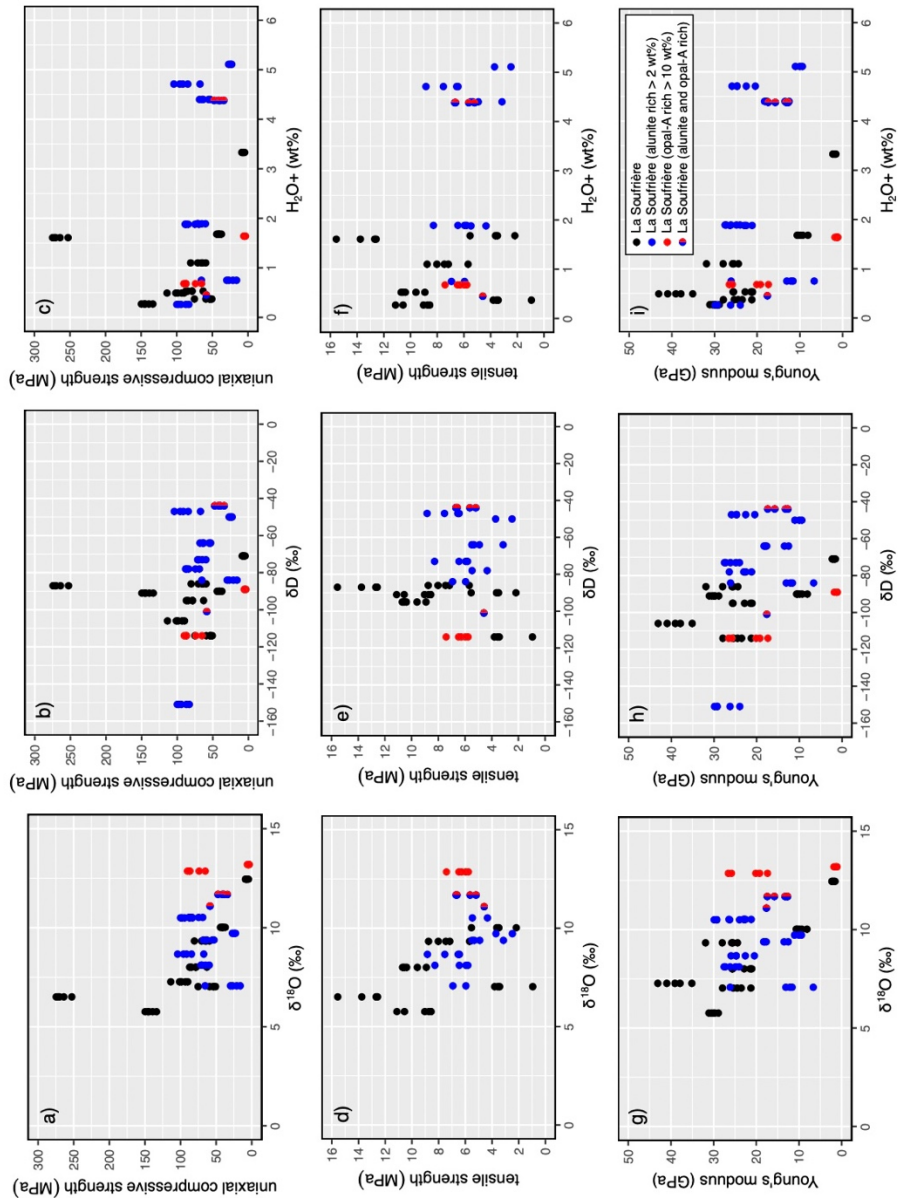
407 **Fig. 1.** Google Earth image (Google Maxar Technologies CNES / Airbus) of La Soufrière de Guadeloupe (Eastern
 408 Caribbean) showing the sampling locations for the 19 rock blocks collected for this study (see text for details).
 409 Whole-rock $\delta^{18}\text{O}$ values, measured in this study (Table 2) are given next to sampling location. Inset shows a map
 410 of Guadeloupe in which the location of La Soufrière de Guadeloupe is indicated by a red triangle.

411



412

413 **Fig. 2.** Whole-rock $\delta^{18}\text{O}$ value (a), whole-rock δD value (b), and water content (c) as a function of the wt% of
 414 secondary minerals for rocks from La Soufrière de Guadeloupe (Eastern Caribbean; sulfate-rich samples (≥ 2 wt%)
 415 are blue, opal-rich samples (≥ 10 wt%) are red, samples that are both sulfate- and opal-rich are blue and red, and
 416 all other samples are black) (alteration data from Heap et al., 2021a, 2022a, b). Photographs of 20 mm-diameter
 417 cylindrical samples cored from selected blocks (those that preserve different degrees of alteration) are provided in
 418 panel (a). Experimental errors are within the size of the symbols. All these data are provided in an Excel®
 419 spreadsheet that accompanies this contribution as Supplementary Information.



420

421

422 **Fig. 3.** Uniaxial compressive strength as a function of $\delta^{18}\text{O}$ value (a), δD value (b), and water content (c) for rocks

423 from La Soufrière de Guadeloupe (Eastern Caribbean; sulfate-rich samples (≥ 2 wt%) are blue, opal-rich samples

424 (≥ 10 wt%) are red, samples that are both sulfate- and opal-rich are blue and red, and all other samples are black).

425 Indirect tensile strength as a function of $\delta^{18}\text{O}$ value (d), δD value (e), and water content (f). Young's modulus as a

426 function of $\delta^{18}\text{O}$ value (g), δD value (h), and water content (i). The strength (compressive and tensile) and Young's

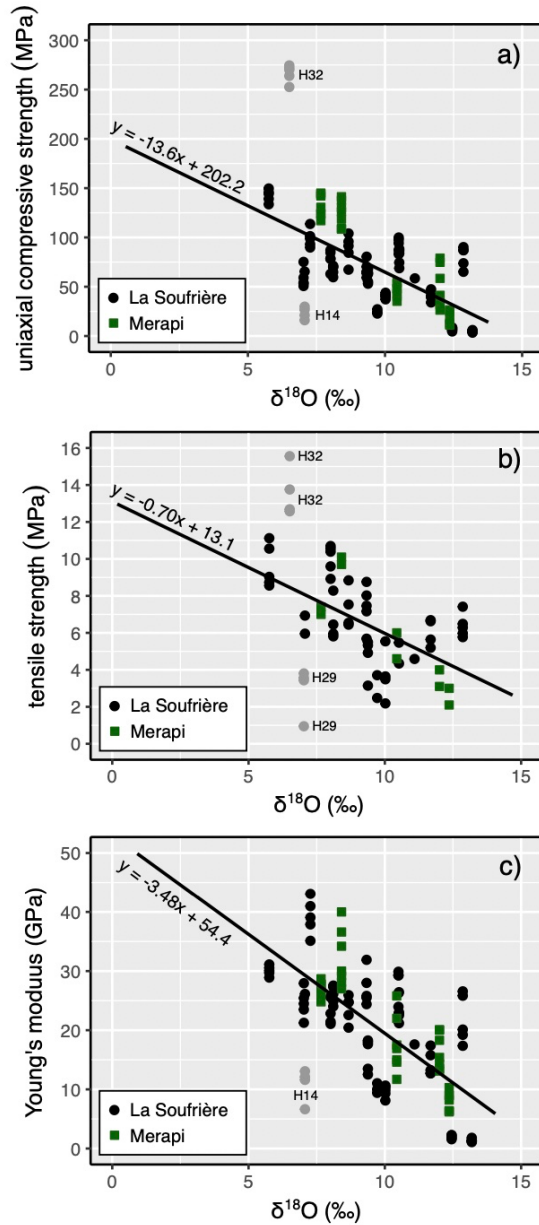
427 modulus data are taken from Heap et al. (2021a, 2022a). Uniaxial compressive strength, tensile strength, and

428 Young's modulus were measured on multiple core samples prepared from each block, which is characterised by a

429 single $\delta^{18}\text{O}$ value, δD value, and water content. Experimental errors are within the size of the symbols. All these

430 data are provided in an Excel® spreadsheet that accompanies this contribution as Supplementary Information.

431



432
 433 **Fig. 4.** Uniaxial compressive strength (a), indirect tensile strength (b), and Young's modulus (c) as a function of
 434 whole-rock $\delta^{18}\text{O}$ values for rocks from La Soufrière de Guadeloupe (Eastern Caribbean; black circles; strength
 435 and Young's modulus data from Heap et al., 2021a, 2022a) and Merapi volcano (Indonesia; green squares; data
 436 from Heap et al., 2019, 2022a; Darmawan et al., 2022). Data outliers are shown in grey (see text for details). Black
 437 lines – best-fit linear functions, Eqs. (1), (2), and (3) for the La Soufrière de Guadeloupe and Merapi volcano data
 438 (excluding the outliers shown in grey). The coefficient of determination for the data of panels (a), (b), and (c) are
 439 0.52, 0.36, and 0.52, respectively. Uniaxial compressive strength, tensile strength, and Young's modulus were
 440 measured on multiple core samples prepared from each block, which is characterised by a single $\delta^{18}\text{O}$ value.
 441 Experimental errors are within the size of the symbols. All these data are provided in an Excel® spreadsheet that
 442 accompanies this contribution as Supplementary Information.

Mineral	H2 A	H2 B	H3	H4 A	H5 A	H6	H1 4	H1 5	H1 8	H1 9	H2 0	H2 1	H2 2	H2 5	H2 9	H3 0	H3 2	WP128 5	WP131 7
Plagioclase	56.7	12.3	46.6	23.3	41.3	30.0	60.7	22.5	61.2	22.0	28.7	24.2	59.5	38.7	62.4	8.9	64.4	64.7	61.6
Clinopyroxene	8.7	3.4	5.6	4.9	5.2	6.4	6.3	7.3	8.4	5.0	8.9	12.4	8.9	5.3	7.8	2.5	9.5	5.2	5.9
Orthopyroxene	10.8	9.5	11.8	11.8	11.1	10.8	8.6	9.2	12.2	10.2	15.0	19.3	13.6	10.2	11.2	3.3	15.1	13.2	15.6
(Ti-) Magnetite	0.7	-	0.8	-	-	-	0.8	-	2.9	-	2.4	3.1	0.8	-	2.7	-	4.9	3.5	0.7
Quartz*	1.0	0.5	0.6	0.6	0.5	0.5	1.7	0.7	0.7	1.7	0.3	0.2	0.6	0.3	0.4	0.9	0.3	0.2	0.7
Cristobalite*	11.3	12.8	10.6	11.8	13.0	11.1	13.5	10.2	11.7	9.5	11.4	11.7	10.6	9.8	12.4	9	5.7	-	-
Tridymite*	-	-	-	-	-	-	-	0.7	-	-	-	-	-	-	-	-	-	13.2	13.2
Hematite*	-	-	-	-	-	-	3.4	-	2.8	2.4	-	-	-	-	3.1	4.3	-	-	-
Pyrite*	3.5	-	3.8	2.3	-	-	-	-	-	-	-	0.4	3.1	0.6	-	-	-	-	-
Alunite*	-	-	-	-	-	-	-	-	-	-	-	-	-	-	-	-	-	-	2.4
Na-Alunite*	1.4	1.6	2.8	1.3	5.4	5.1	5.1	15.0	-	14.2	0.5	0.5	-	9.8	-	25.6	-	-	-
Gypsum*	-	-	-	0.7	-	-	-	-	-	-	0.8	1.2	-	-	-	-	-	-	-
Kaolinite*	6	59.7	17.4	43.3	23.5	36.0	<1	34.3	-	2.0	2.0	2.0	<1	25.3	-	35.6	-	-	-
Talc*	-	-	-	-	-	-	-	-	-	-	-	-	2.9	-	-	-	-	-	-
Opal-A*	-	-	-	-	-	-	-	-	-	33	30	25	-	-	-	10	-	-	-

443

444 **Table 1.** Mineral contents of the 19 rock blocks from La Soufrière de Guadeloupe measured by X-ray powder
445 diffraction. Values in wt%. Asterisk denotes a secondary mineral (i.e. alteration mineral). Data for H30 and H32
446 were published in Heap et al. (2022b). All other data were published in Heap et al. (2021a). The relative errors in
447 the quantification are in the order of 5–10%.

448

Volcano	Block	Weight percentage of secondary minerals	$\delta^{18}\text{O}$ (‰)	δD (‰)	H_2O^+ (wt%)
La Soufrière	H2A	23	9.3	-86	1.1
La Soufrière	H2B	75	12.5	-71	3.3
La Soufrière	H3	35	8.1	-73	1.9
La Soufrière	H4A	60	10.0	-90	1.7
La Soufrière	H5A	42	10.5	-78	1.9
La Soufrière	H6	53	9.4	-64	4.4
La Soufrière	H14	24	7.1	-84	0.8
La Soufrière	H15	61	9.7	-50	5.1
La Soufrière	H18	15	7.3	-106	0.5
La Soufrière	H19	63	11.7	-44	4.4
La Soufrière	H20	45	13.2	-89	1.6
La Soufrière	H21	41	12.9	-114	0.7
La Soufrière	H22	17	5.8	-91	0.3
La Soufrière	H25	46	10.5	-151	0.3
La Soufrière	H29	16	7.0	-114	0.4
La Soufrière	H30	85	11.1	-101	0.5
La Soufrière	H32	6	6.5	-87	1.6
La Soufrière	WP1285	13	8.0	-95	0.5
La Soufrière	WP1317	16	8.7	-47	4.7
Merapi	MU	8	7.7	NA	NA
Merapi	MSA1	33	12.4	NA	NA
Merapi	MSA2	29	8.4	NA	NA
Merapi	MHA1	45	10.4	NA	NA
Merapi	MHA2	62	12.0	NA	NA

449

450 **Table 2.** The weight percentage of secondary minerals (data from Heap et al., 2021a, 2022a, b), whole-rock $\delta^{18}\text{O}$
451 values, whole-rock δD values, and water content (H_2O^+) for rocks from La Soufrière de Guadeloupe (Eastern
452 Caribbean) and Merapi volcano (Indonesia; data from Darmawan et al., 2022; Heap et al., 2019, 2022a). The
453 sampling locations for the blocks from La Soufrière de Guadeloupe are shown in Fig. 1. NA – not analysed

454

455 **References**

- 456 Ahmed, A. S., Revil, A., Byrdina, S., Coperey, A., Gailler, L., Grobde, N., ... & Humaida, H. (2018). 3D electrical
457 conductivity tomography of volcanoes. *Journal of Volcanology and Geothermal Research*, 356, 243-263.
- 458 Aizawa, K., Ogawa, Y., & Ishido, T. (2009). Groundwater flow and hydrothermal systems within volcanic
459 edifices: Delineation by electric self-potential and magnetotellurics. *Journal of Geophysical Research: Solid
460 Earth*, 114(B1).
- 461 Apuani, T., Corazzato, C., Cancelli, A., & Tibaldi, A. (2005). Stability of a collapsing volcano (Stromboli, Italy):
462 Limit equilibrium analysis and numerical modelling. *Journal of Volcanology and Geothermal Research*,
463 144(1-4), 191-210.
- 464 Ball, J. L., Stauffer, P. H., Calder, E. S., & Valentine, G. A. (2015). The hydrothermal alteration of cooling lava
465 domes. *Bulletin of Volcanology*, 77(12), 1-16.
- 466 Ball, J. L., Taron, J., Reid, M. E., Hurwitz, S., Finn, C., & Bedrosian, P. (2018). Combining multiphase
467 groundwater flow and slope stability models to assess stratovolcano flank collapse in the Cascade Range.
468 *Journal of Geophysical Research: Solid Earth*, 123(4), 2787-2805.
- 469 Belousov, A., Voight, B., & Belousova, M. (2007). Directed blasts and blast-generated pyroclastic density
470 currents: a comparison of the Bezymianny 1956, Mount St Helens 1980, and Soufrière Hills, Montserrat
471 1997 eruptions and deposits. *Bulletin of Volcanology*, 69(7), 701-740.
- 472 Berg, S. E., Troll, V. R., Harris, C., Deegan, F. M., Riisshuus, M. S., Burchardt, S., & Krumbholz, M. (2018).
473 Exceptionally high whole-rock $\delta^{18}\text{O}$ values in intra-caldera rhyolites from Northeast Iceland.
474 *Mineralogical Magazine*, 82(5), 1147-1168.
- 475 Bergmann, J., Friedel, P., & Kleeberg, R. (1998). BGMN—a new fundamental parameters based Rietveld program
476 for laboratory X-ray sources, its use in quantitative analysis and structure investigations. *CPD Newsletter*,
477 20(5).
- 478 Bindeman, I. (2008). Oxygen isotopes in mantle and crustal magmas as revealed by single crystal analysis.
479 *Reviews in Mineralogy and Geochemistry*, 69(1), 445-478.
- 480 Borthwick, J., & Harmon, R. S. (1982). A note regarding CIF3 as an alternative to BrF5 for oxygen isotope
481 analysis. *Geochimica et Cosmochimica Acta*, 46(9), 1665-1668.
- 482 Boudon, G., Le Friant, A., Villemant, B., Viodé, J.-P. (2005). Martinique. In: Lindsay, J.M., Robertson, R.E.A.,
483 Shepherd, J.B., Ali, S. (Eds.), *Volcanic Hazard Atlas of the Lesser Antilles*. Seismic Research Uni, The
484 University of the West Indies, Trinidad and Tobago, WI, pp. 126–145.
- 485 Boudon, G., Le Friant, A., Komorowski, J. C., Deplus, C., & Semet, M. P. (2007). Volcano flank instability in the
486 Lesser Antilles Arc: Diversity of scale, processes, and temporal recurrence. *Journal of Geophysical
487 Research: Solid Earth*, 112(B8).
- 488 Brandriss, M.E., O'Neil, J.R., Edlund, M.B., Stoermer, E.F. (1998) Oxygen isotope fractionation between
489 diatomaceous silica and water. *Geochimica et Cosmochimica Acta*, 62(7), 119-1125.
- 490 Brombach, T., Marini, L., & Hunziker, J. C. (2000). Geochemistry of the thermal springs and fumaroles of Basse-
491 Terre Island, Guadeloupe, Lesser Antilles. *Bulletin of Volcanology*, 61(7), 477-490.
- 492 Browne, P. R. L. (1978). Hydrothermal alteration in active geothermal fields. *Annual review of earth and planetary
493 sciences*, 6(1), 229-248.
- 494 Byrdina, S., Friedel, S., Vandemeulebrouck, J., Budi-Santoso, A., Suryanto, W., Rizal, M. H., & Winata, E. (2017).
495 Geophysical image of the hydrothermal system of Merapi volcano. *Journal of Volcanology and Geothermal
496 Research*, 329, 30-40.
- 497 Byrdina, S., Grandis, H., Sumintadireja, P., Caudron, C., Syahbana, D. K., Naffrechoux, E., ... &
498 Vandemeulebrouck, J. (2018). Structure of the acid hydrothermal system of Papandayan volcano,
499 Indonesia, investigated by geophysical methods. *Journal of Volcanology and Geothermal Research*, 358,
500 77-86.
- 501 Carlut, J., & Quidelleur, X. (2000). Absolute paleointensities recorded during the Brunhes chron at La Guadeloupe
502 Island. *Physics of the Earth and Planetary Interiors*, 120(4), 255-269.
- 503 Cant, J. L., Siratovich, P. A., Cole, J. W., Villeneuve, M. C., & Kennedy, B. M. (2018). Matrix permeability of
504 reservoir rocks, Ngatamariki geothermal field, Taupo Volcanic Zone, New Zealand. *Geothermal Energy*,
505 6(1), 1-28.
- 506 Cathles, L. M. (1993). Oxygen isotope alteration in the Noranda mining district, Abitibi greenstone belt, Quebec.
507 *Economic Geology*, 88(6), 1483-1511.
- 508 Cecchi, E., de Vries, B. V. W., & Lavest, J. M. (2004). Flank spreading and collapse of weak-cored volcanoes.
509 *Bulletin of Volcanology*, 67(1), 72-91.
- 510 Chiodini, G., Cioni, R., Frullani, A., Guidi, M., Marini, L., Prati, F., & Raco, B. (1996). Fluid geochemistry of
511 Montserrat Island, West Indies. *Bulletin of Volcanology*, 58(5), 380-392.

- 512 Criss, R. E., Champion, D. E., & McIntyre, D. H. (1985). Oxygen isotope, aeromagnetic, and gravity anomalies
513 associated with hydrothermally altered zones in the Yankee Fork mining district, Custer County, Idaho.
514 *Economic Geology*, 80(5), 1277-1296.
- 515 Darmawan, H., Troll, V. R., Walter, T. R., Deegan, F. M., Geiger, H., Heap, M. J., ... & Müller, D. (2022). Hidden
516 mechanical weaknesses within lava domes provided by buried high-porosity hydrothermal alteration zones.
517 *Scientific Reports*, 12(1), 1-14.
- 518 Davidson, J. (1985). Mechanisms of contamination in Lesser Antilles island arc magmas from radiogenic and
519 oxygen isotope relationships. *Earth and Planetary Science Letters*, 72(2-3), 163-174.
- 520 Davidson, J. P., & Harmon, R. S. (1989). Oxygen isotope constraints on the petrogenesis of volcanic arc magmas
521 from Martinique, Lesser Antilles. *Earth and Planetary Science Letters*, 95(3-4), 255-270.
- 522 Day, S. J. (1996). Hydrothermal pore fluid pressure and the stability of porous, permeable volcanoes. *Geological*
523 *Society, London, Special Publications*, 110(1), 77-93.
- 524 Deegan, F. M., Whitehouse, M. J., Troll, V. R., Geiger, H., Jeon, H., le Roux, P., ... & González-Maurel, O. (2021).
525 Sunda arc mantle source $\delta^{18}\text{O}$ value revealed by intracrystal isotope analysis. *Nature Communications*,
526 12(1), 1-10.
- 527 del Potro, R., & Hürliemann, M. (2009). The decrease in the shear strength of volcanic materials with argillic
528 hydrothermal alteration, insights from the summit region of Teide stratovolcano, Tenerife. *Engineering*
529 *Geology*, 104(1-2), 135-143.
- 530 Donoghue, E., Troll, V. R., Harris, C., O'Halloran, A., Walter, T. R., & Torrado, F. J. P. (2008). Low-temperature
531 hydrothermal alteration of intra-caldera tuffs, Miocene Tejeda caldera, Gran Canaria, Canary Islands.
532 *Journal of Volcanology and Geothermal Research*, 176(4), 551-564.
- 533 Donoghue, E., Troll, V. R., & Harris, C. (2010). Hydrothermal alteration of the Miocene Tejeda Intrusive
534 Complex, Gran Canaria, Canary Islands: insights from petrography, mineralogy and O- and H- isotope
535 geochemistry. *Journal of Petrology*, 51, 2149-2176.
- 536 Farquharson, J. I., Wild, B., Kushnir, A. R., Heap, M. J., Baud, P., & Kennedy, B. (2019). Acid-induced dissolution
537 of andesite: evolution of permeability and strength. *Journal of Geophysical Research: Solid Earth*, 124(1),
538 257-273.
- 539 Finizola, A., Ricci, T., Deiana, R., Cabusson, S. B., Rossi, M., Praticelli, N., ... & Lelli, M. (2010). Adventive
540 hydrothermal circulation on Stromboli volcano (Aeolian Islands, Italy) revealed by geophysical and
541 geochemical approaches: implications for general fluid flow models on volcanoes. *Journal of Volcanology*
542 *and Geothermal Research*, 196(1-2), 111-119.
- 543 Finn, C. A., Deszcz-Pan, M., Ball, J. L., Bloss, B. J., & Minsley, B. J. (2018). Three-dimensional geophysical
544 mapping of shallow water saturated altered rocks at Mount Baker, Washington: Implications for slope
545 stability. *Journal of Volcanology and Geothermal Research*, 357, 261-275.
- 546 Finn, C.A., Bedrosian, P.A., Holbrook, W.S., Auken, E., Bloss, B. R., & Crosbie J. (2022). Geophysical imaging
547 of the Yellowstone hydrothermal plumbing system. *Nature* 603, 643–647.
- 548 Frolova, J., Ladygin, V., Rychagov, S., & Zukhubaya, D. (2014). Effects of hydrothermal alterations on physical
549 and mechanical properties of rocks in the Kuril–Kamchatka island arc. *Engineering Geology*, 183, 80-95.
- 550 Fulignati, P. (2020). Clay minerals in hydrothermal systems. *Minerals*, 10(10), 919.
- 551 Gonfiantini, R. (1978). Standards for stable isotope measurements in natural compounds. *Nature*, 271(5645), 534-
552 536.
- 553 Ghorbani, A., Revil, A., Coperey, A., Ahmed, A. S., Roque, S., Heap, M. J., ... & Viveiros, F. (2018). Complex
554 conductivity of volcanic rocks and the geophysical mapping of alteration in volcanoes. *Journal of*
555 *Volcanology and Geothermal Research*, 357, 106-127.
- 556 Green, G. R., Ohmoto, H., Date, J., & Takahashi, T. (1983). Whole-rock oxygen isotope distribution in the
557 Fukazawa-Kosaka area, Hokuroku District, Japan, and its potential application to mineral exploration. In:
558 *Economic Geology Monograph 5 The Kuroko and Related Volcanogenic Massive Sulfide Deposits* (Eds:
559 Ohmoto, H. & Skinner B. J.). DOI: <https://doi.org/10.5382/Mono.05.24>.
- 560 Hansteen, T. H., & Troll, V. R. (2003). Oxygen isotope composition of xenoliths from the oceanic crust and
561 volcanic edifice beneath Gran Canaria (Canary Islands): consequences for crustal contamination of
562 ascending magmas. *Chemical Geology*, 193(3-4), 181-193.
- 563 Harnett, C. E., & Heap, M. J. (2021). Mechanical and topographic factors influencing lava dome growth and
564 collapse. *Journal of Volcanology and Geothermal Research*, 420, 107398.
- 565 Harris, C., Compton, J. S., & Bevington, S. A. (1999). Oxygen and hydrogen isotope composition of kaolinite
566 deposits, Cape Peninsula, South Africa; low-temperature, meteoric origin. *Economic Geology*, 94(8), 1353-
567 1366.
- 568 Harris, C., & Vogeli, J. (2010). Oxygen isotope composition of garnet in the Peninsula Granite, Cape Granite
569 Suite, South Africa: constraints on melting and emplacement mechanisms. *South African Journal of*
570 *Geology*, 113(4), 401-412.

- 571 Hattori, K., & Muehlenbachs, K. (1982). Oxygen isotope ratios of the Icelandic crust. *Journal of Geophysical*
572 *Research: Solid Earth*, 87(B8), 6559-6565.
- 573 Heap, M. J., Troll, V. R., Kushnir, A. R., Gilg, H. A., Collinson, A. S., Deegan, F. M., ... & Walter, T. R. (2019).
574 Hydrothermal alteration of andesitic lava domes can lead to explosive volcanic behaviour. *Nature*
575 *Communications*, 10(1), 1-10.
- 576 Heap, M. J., Villeneuve, M., Albino, F., Farquharson, J. I., Brothelande, E., Amelung, F., ... & Baud, P. (2020a).
577 Towards more realistic values of elastic moduli for volcano modelling. *Journal of volcanology and*
578 *geothermal research*, 390, 106684.
- 579 Heap, M. J., Gravley, D. M., Kennedy, B. M., Gilg, H. A., Bertolett, E., & Barker, S. L. (2020b). Quantifying the
580 role of hydrothermal alteration in creating geothermal and epithermal mineral resources: the Ohakuri
581 ignimbrite (Taupō Volcanic Zone, New Zealand). *Journal of Volcanology and Geothermal Research*, 390,
582 106703.
- 583 Heap, M. J., Baumann, T. S., Rosas-Carbajal, M., Komorowski, J. C., Gilg, H. A., Villeneuve, M., ... & Reuschlé,
584 T. (2021a). Alteration-Induced Volcano Instability at La Soufrière de Guadeloupe (Eastern Caribbean).
585 *Journal of Geophysical Research: Solid Earth*, 126(8), e2021JB022514.
- 586 Heap, M. J., Baumann, T., Gilg, H. A., Kolzenburg, S., Ryan, A. G., Villeneuve, M., ... & Clynne, M. A. (2021b).
587 Hydrothermal alteration can result in pore pressurization and volcano instability. *Geology*, 49(11), 1348-
588 1352.
- 589 Heap, M. J., & Violay, M. E. (2021). The mechanical behaviour and failure modes of volcanic rocks: a review.
590 *Bulletin of Volcanology*, 83(5), 1-47.
- 591 Heap, M. J., Harnett, C. E., Wadsworth, F. B., Gilg, H. A., Carbillet, L., Rosas-Carbajal, M., Komorowski, J.- C.,
592 Baud, P., Troll, V. R., Deegan, F. M., Holohan, E. P., & Moretti, R. (2022a). The tensile strength of
593 hydrothermally altered volcanic rocks. *Journal of Volcanology and Geothermal Research*, 428, 107576.
594 DOI: 10.1016/j.jvolgeores.2022.107576.
- 595 Heap, M. J., Jessop, D. E., Wadsworth, F. B., Rosas-Carbajal, M., Komorowski, J. C., Gilg, H. A., ... & Moretti,
596 R. (2022b). The thermal properties of hydrothermally altered andesites from La Soufrière de Guadeloupe
597 (Eastern Caribbean). *Journal of Volcanology and Geothermal Research*, 421, 107444.
- 598 Hoblitt, R. P., Miller, C. D., & Vallance, J. W. (1981). Origin and stratigraphy of the deposit produced by the May
599 18 directed blast. In *The 1980 Eruptions of Mount St. Helens, Washington* (Vol. 1250, pp. 401-419). US
600 Government Printing Office Washington, DC.
- 601 Hoek, E., Carranza-Torres, C., & Corkum, B. (2002). Hoek-Brown failure criterion-2002 edition. *Proceedings of*
602 *NARMS-Tac*, 1(1), 267-273.
- 603 Hoek, E., & Diederichs, M. S. (2006). Empirical estimation of rock mass modulus. *International journal of rock*
604 *mechanics and mining sciences*, 43(2), 203-215.
- 605 Inoue, A. (1995). Formation of clay minerals in hydrothermal environments. In *Origin and mineralogy of clays*
606 (pp. 268-329). Springer, Berlin, Heidelberg.
- 607 Jessop, D. E., Moune, S., Moretti, R., Gibert, D., Komorowski, J. C., Robert, V., ... & Burtin, A. (2021). A multi-
608 decadal view of the heat and mass budget of a volcano in unrest: La Soufrière de Guadeloupe (French West
609 Indies). *Bulletin of Volcanology*, 83(3), 1-19.
- 610 Joseph, E. P., Fournier, N., Lindsay, J. M., & Fischer, T. P. (2011). Gas and water geochemistry of geothermal
611 systems in Dominica, Lesser Antilles island arc. *Journal of Volcanology and Geothermal Research*, 206(1-
612 2), 1-14.
- 613 Kereszturi, G., Schaefer, L., Mead, S., Miller, C., Procter, J., & Kennedy, B. (2021). Synthesis of hydrothermal
614 alteration, rock mechanics and geophysical mapping to constrain failure and debris avalanche hazards at
615 Mt. Ruapehu (New Zealand). *New Zealand Journal of Geology and Geophysics*, 64(2-3), 421-442.
- 616 Kita, I., Taguchi, S., & Matsubaya, O. (1985). Oxygen isotope fractionation between amorphous silica and water
617 at 34–93 °C. *Nature*, 314(6006), 83-84.
- 618 Komorowski J.-C., Boudon G., Semet, M., Beauducel, F., Anténor-Habazac, C., Bazin, S., Hammmouya, G.
619 (2005). Guadeloupe. J. Lindsay, R. Robertson, J. Shepherd, S. Ali (Eds.), *Volcanic Atlas of the Lesser*
620 *Antilles*, University of the French West Indies, Seismic Research Unit, 65-102.
- 621 Komorowski, J.-C., Legendre, Y., Boudon, G., Barsotti, S., Esposti-Ongaro, T., Jenkins, S., et al. (2012). A new
622 Holocene eruptive chronology for la Soufrière de Guadeloupe volcano: implications for credible scenario
623 definition as well as hazard and impact modelling, Colima, Mexico: *Cities on Volcanoes*, IAVCEI, 7, 18–
624 23.
- 625 Komorowski, J. C., Jenkins, S., Baxter, P. J., Picquout, A., Lavigne, F., Charbonnier, S., ... & Budi-Santoso, A.
626 (2013). Paroxysmal dome explosion during the Merapi 2010 eruption: processes and facies relationships of
627 associated high-energy pyroclastic density currents. *Journal of Volcanology and Geothermal Research*, 261,
628 260-294.

- 629 Le Friant, A., Boudon, G., Komorowski, J. C., Heinrich, P., & Semet, M. P. (2006). Potential flank-collapse of
630 Soufriere Volcano, Guadeloupe, lesser Antilles? Numerical simulation and hazards. *Natural hazards*, 39(3),
631 381-393.
- 632 Legendre, Y. (2012). Reconstruction fine de l'histoire éruptive et scenarii éruptifs à la soufrière de Guadeloupe:
633 vers un modèle intégré de fonctionnement du volcan (Doctoral dissertation, Paris 7).
- 634 Lentz, D. R. (1999). Petrology, geochemistry, and oxygen isotope interpretation of felsic volcanic and related
635 rocks hosting the Brunswick 6 and 12 massive sulfide deposits (Brunswick Belt), Bathurst mining camp,
636 New Brunswick, Canada. *Economic Geology*, 94(1), 57-86.
- 637 Lévy, L., Gibert, B., Sigmundsson, F., Flóvenz, Ó. G., Hersir, G. P., Briole, P., & Pezard, P. A. (2018). The role
638 of smectites in the electrical conductivity of active hydrothermal systems: electrical properties of core
639 samples from Krafla volcano, Iceland. *Geophysical Journal International*, 215(3), 1558-1582.
- 640 Lipman, P. W., & Mullineaux, D. R. (1981). The 1980 eruptions of Mount St. Helens, Washington (No. 1250).
641 USGPO.
- 642 Lube, G., Breard, E. C., Cronin, S. J., Procter, J. N., Brenna, M., Moebis, A., ... & Fournier, N. (2014). Dynamics
643 of surges generated by hydrothermal blasts during the 6 August 2012 Te Maari eruption, Mt. Tongariro,
644 New Zealand. *Journal of Volcanology and Geothermal Research*, 286, 348-366.
- 645 Marmoni, G. M., Martino, S., Heap, M. J., & Reuschlé, T. (2017). Gravitational slope-deformation of a resurgent
646 caldera: New insights from the mechanical behaviour of Mt. Nuovo tuffs (Ischia Island, Italy). *Journal of
647 Volcanology and Geothermal Research*, 345, 1-20.
- 648 Mayer, K., Scheu, B., Montanaro, C., Yilmaz, T. I., Isaia, R., Aßbichler, D., & Dingwell, D. B. (2016).
649 Hydrothermal alteration of surficial rocks at Solfatara (Campi Flegrei): Petrophysical properties and
650 implications for phreatic eruption processes. *Journal of Volcanology and Geothermal Research*, 320, 128-
651 143.
- 652 Metcalfe, A., Moune, S., Komorowski, J. C., Kilgour, G., Jessop, D. E., Moretti, R., & Legendre, Y. (2021).
653 Magmatic Processes at La Soufrière de Guadeloupe: Insights From Crystal Studies and Diffusion
654 Timescales for Eruption Onset. *Frontiers in Earth Science*, 9, 78.
- 655 Moon, V., Bradshaw, J., Smith, R., & de Lange, W. (2005). Geotechnical characterisation of stratocone crater wall
656 sequences, White Island Volcano, New Zealand. *Engineering geology*, 81(2), 146-178.
- 657 Mordensky, S. P., Heap, M. J., Kennedy, B. M., Gilg, H. A., Villeneuve, M. C., Farquharson, J. I., & Gravley, D.
658 M. (2019). Influence of alteration on the mechanical behaviour and failure mode of andesite: implications
659 for shallow seismicity and volcano monitoring. *Bulletin of Volcanology*, 81(8), 1-12.
- 660 Mordensky, S. P., Villeneuve, M. C., Kennedy, B. M., & Struthers, J. (2022). Hydrothermally induced edifice
661 destabilisation: The mechanical behaviour of rock mass surrounding a shallow intrusion in andesitic lavas,
662 Pinnacle Ridge, Ruapehu (New Zealand). *Engineering Geology*, 106696.
- 663 Moretti, R., Komorowski, J. C., Ucciani, G., Moune, S., Jessop, D., de Chabaliér, J. B., ... & Chaussidon, M.
664 (2020). The 2018 unrest phase at La Soufrière of Guadeloupe (French West Indies) andesitic volcano:
665 Scrutiny of a failed but prodromal phreatic eruption. *Journal of Volcanology and Geothermal Research*,
666 393, 106769.
- 667 Moretti, R., Moune, S., Jessop, D., Glynn, C., Robert, V., & Deroussi, S. (2021). The Basse-Terre Island of
668 Guadeloupe (Eastern Caribbean, France) and Its Volcanic-Hydrothermal Geodiversity: A Case Study of
669 Challenges, Perspectives, and New Paradigms for Resilience and Sustainability on Volcanic Islands.
670 *Geosciences*, 11(11), 454.
- 671 Moune, S., Moretti, R., Burtin, A., Jessop, D., Didier, T., Robert, V., ... & Buscetti, M. (2022). Gas monitoring of
672 volcanic-hydrothermal plumes in a tropical environment: the case of La Soufriere de Guadeloupe unrest
673 volcano (Lesser Antilles). *Front. Earth Sci.*, 10, 795760.
- 674 Okubo, C. H. (2004). Rock mass strength and slope stability of the Hilina slump, Kilauea volcano, Hawai'i. *Journal
675 of Volcanology and Geothermal Research*, 138(1-2), 43-76.
- 676 Paradis, S., Taylor, B. E., Watkinson, D. H., & Jonasson, I. R. (1993). Oxygen isotope zonation and alteration in
677 the northern Noranda District, Quebec; evidence for hydrothermal fluid flow. *Economic Geology*, 88(6),
678 1512-1525.
- 679 Peruzzetto, M., Komorowski, J. C., Le Friant, A., Rosas-Carbajal, M., Mangeney, A., & Legendre, Y. (2019).
680 Modeling of partial dome collapse of La Soufrière of Guadeloupe volcano: implications for hazard
681 assessment and monitoring. *Scientific reports*, 9(1), 1-15.
- 682 Reid, M. E., Sisson, T. W., & Brien, D. L. (2001). Volcano collapse promoted by hydrothermal alteration and
683 edifice shape, Mount Rainier, Washington. *Geology*, 29(9), 779-782.
- 684 Reid, M. E. (2004). Massive collapse of volcano edifices triggered by hydrothermal pressurization. *Geology*,
685 32(5), 373-376.
- 686 Rosas-Carbajal, M., Komorowski, J. C., Nicollin, F., & Gibert, D. (2016). Volcano electrical tomography unveils
687 edifice collapse hazard linked to hydrothermal system structure and dynamics. *Scientific reports*, 6(1), 1-
688 11.

- 689 Rose, T. P., Criss, R. E., Mughannam, A. J., & Clynne, M. A. (1994). Oxygen isotope evidence for hydrothermal
690 alteration within a Quaternary stratovolcano, Lassen Volcanic National Park, California. *Journal of*
691 *Geophysical Research: Solid Earth*, 99(B11), 21621-21633.
- 692 Rye, R. O. (2005). A review of the stable-isotope geochemistry of sulfate minerals in selected igneous
693 environments and related hydrothermal systems. *Chemical Geology*, 215(1-4), 5-36.
- 694 Salaün, A., Villemant, B., Gérard, M., Komorowski, J. C., & Michel, A. (2011). Hydrothermal alteration in
695 andesitic volcanoes: trace element redistribution in active and ancient hydrothermal systems of Guadeloupe
696 (Lesser Antilles). *Journal of Geochemical Exploration*, 111(3), 59-83.
- 697 Schaefer, L. N., Kereszturi, G., Villeneuve, M., & Kennedy, B. (2021). Determining physical and mechanical
698 volcanic rock properties via reflectance spectroscopy. *Journal of Volcanology and Geothermal Research*,
699 420, 107393.
- 700 Scher, S., Williams-Jones, A. E., & Williams-Jones, G. (2013). Fumarolic activity, acid-sulfate alteration, and high
701 sulfidation epithermal precious metal mineralization in the crater of Kawah Ijen Volcano, Java, Indonesia.
702 *Economic Geology*, 108(5), 1099-1118.
- 703 Sheppard, S. M. F., & Gilg, H. A. (1996). Stable isotope geochemistry of clay minerals: "The story of sloppy,
704 sticky, lumpy and tough" Cairns-Smith (1971). *Clay minerals*, 31(1), 1-24.
- 705 Siratovich, P. A., Heap, M. J., Villeneuve, M. C., Cole, J. W., & Reuschlé, T. (2014). Physical property
706 relationships of the Rotokawa Andesite, a significant geothermal reservoir rock in the Taupo Volcanic
707 Zone, New Zealand. *Geothermal Energy*, 2(1), 1-31.
- 708 Sparks, R. S. J., Barclay, J., Calder, E. S., Herd, R. A., Komorowski, J. C., Luckett, R., ... & Woods, A. W. (2002).
709 Generation of a debris avalanche and violent pyroclastic density current on 26 December (Boxing Day)
710 1997 at Soufriere Hills Volcano, Montserrat. *Geological Society, London, Memoirs*, 21(1), 409-434.
- 711 Stoffregen, R. E., Rye, R. O., & Wasserman, M. D. (1994). Experimental studies of alunite: I. 18O-16O and DH
712 fractionation factors between alunite and water at 250–450 C. *Geochimica et Cosmochimica Acta*, 58(2),
713 903-916.
- 714 Taylor, H. P. (1974). The application of oxygen and hydrogen isotope studies to problems of hydrothermal
715 alteration and ore deposit. *Economic Geology*, 69(843,883).
- 716 Troll, V. R., Hilton, D. R., Jolis, E. M., Chadwick, J. P., Blythe, L. S., Deegan, F. M., ... & Zimmer, M. (2012).
717 Crustal CO₂ liberation during the 2006 eruption and earthquake events at Merapi volcano, Indonesia.
718 *Geophysical Research Letters*, 39(11).
- 719 Tseng, K. H., Ogawa, Y., Tank, S. B., Ujihara, N., Honkura, Y., Terada, A., ... & Kanda, W. (2020). Anatomy of
720 active volcanic edifice at the Kusatsu–Shirane volcano, Japan, by magnetotellurics: hydrothermal
721 implications for volcanic unrests. *Earth, Planets and Space*, 72(1), 1-11.
- 722 Van Soest, M. C., Hilton, D. R., MacPherson, C. G., & Matthey, D. P. (2002). Resolving sediment subduction and
723 crustal contamination in the Lesser Antilles Island Arc: a combined He–O–Sr isotope approach. *Journal of*
724 *Petrology*, 43(1), 143-170.
- 725 van Wyk de Vries, B., Kerle, N., & Petley, D. (2000). Sector collapse forming at Casita volcano, Nicaragua.
726 *Geology*, 28(2), 167-170.
- 727 Vennemann, T. W., & Smith, H. S. (1990). The rate and temperature of reaction of CIF₃ with silicate minerals,
728 and their relevance to oxygen isotope analysis. *Chemical Geology: Isotope Geoscience section*, 86(1), 83-
729 88.
- 730 Vennemann, T. W., & O'Neil, J. R. (1993). A simple and inexpensive method of hydrogen isotope and water
731 analyses of minerals and rocks based on zinc reagent. *Chemical Geology*, 103(1-4), 227-234.
- 732 Villemant, B., Hammouya, G., Michel, A., Semet, M. P., Komorowski, J. C., Boudon, G., & Cheminée, J. L.
733 (2005). The memory of volcanic waters: shallow magma degassing revealed by halogen monitoring in
734 thermal springs of La Soufrière volcano (Guadeloupe, Lesser Antilles). *Earth and Planetary Science Letters*,
735 237(3-4), 710-728.
- 736 Villemant, B., Komorowski, J. C., Dessert, C., Michel, A., Crispi, O., Hammouya, G., ... & De Chabalière, J. B.
737 (2014). Evidence for a new shallow magma intrusion at La Soufrière of Guadeloupe (Lesser Antilles):
738 insights from long-term geochemical monitoring of halogen-rich hydrothermal fluids. *Journal of*
739 *Volcanology and Geothermal Research*, 285, 247-277.
- 740 Voight, B., Glicken, H., Janda, R. J., & Douglass, P. M. (1981). Catastrophic rockslide avalanche of May 18. US
741 Geological Survey Professional Paper, 1250, 347-377.
- 742 Voight, B., Komorowski, J. C., Norton, G. E., Belousov, A., Belousova, M., Boudon, G., ... & Young, S. (2002).
743 The 1997 Boxing Day sector collapse and debris avalanches, Soufrière Hills volcano, Montserrat, WI. *The*
744 *Eruption of Soufriere Hills Volcano, Montserrat, From 1995 to 1999*, 363-407.
- 745 Wallace, C. S., Schaefer, L. N., & Villeneuve, M. C. (2021). Material Properties and Triggering Mechanisms of
746 an Andesitic Lava Dome Collapse at Shiveluch Volcano, Kamchatka, Russia, Revealed Using the Finite
747 Element Method. *Rock Mechanics and Rock Engineering*, 1-18.

- 748 Watters, R. J., Zimbelman, D. R., Bowman, S. D., & Crowley, J. K. (2000). Rock mass strength assessment and
749 significance to edifice stability, Mount Rainier and Mount Hood, Cascade Range volcanoes. *Pure and*
750 *Applied Geophysics*, 157(6), 957-976.
- 751 Wyering, L. D., Villeneuve, M. C., Wallis, I. C., Siratovich, P. A., Kennedy, B. M., Gravley, D. M., & Cant, J. L.
752 (2014). Mechanical and physical properties of hydrothermally altered rocks, Taupo Volcanic Zone, New
753 Zealand. *Journal of Volcanology and Geothermal Research*, 288, 76-93.
- 754 Zimbelman, D. R., Rye, R. O., & Breit, G. N. (2005). Origin of secondary sulfate minerals on active andesitic
755 stratovolcanoes. *Chemical Geology*, 215(1-4), 37-60.